S^3 SEMISUBMERGED SHIP CONCEPT AND EXPERIMENTAL HYDRODYNAMIC COEFFICIENTS

by

DR. THOMAS G. LANG

Reprinted from

NAVAL ENGINEERS JOURNAL

APRIL, 1972

DR. THOMAS G. LANG

S^3 SEMISUBMERGED SHIP CONCEPT AND EXPERIMENTAL HYDRODYNAMIC COEFFICIENTS

THE AUTHOR

received his Bachelor of Science degrees in Mechanical and Civil Engineering from California Institute of Technology in 1948 and 1950, his M.S. degree in Mechanical Engineering from University of Southern California in 1953, and his PhD. in Aerospace Engineering from Penn State University in 1968. He has been with the Navy Undersea Research and Development Center and the Naval Ordnance Test Station since 1951. His specialty is hydrodynamics, but he also has working experience in structures, mechanical design, and dynamics and control. He is presently Head of the Advanced Concepts Group at NUC, and in the course of his career has over 50 publications, including patents, in the areas of underwater propulsion, vehicle stability and control, hydrofoil theory and experiment, submerged vehicle design, semisubmerged ships, and engineering design theory.

ABSTRACT

The S^3 semisubmerged ship concept consists basically of two parallel torpedo-like hulls, submerged to a depth of one to two hull diameters, and attached to an above-water platform by means of four widely-spaced vertical struts. Horizontal fins on the hulls provide dynamic stability, and control surfaces permit full automatic control over pitch, heave, and roll. Results of a series of towing tank tests conducted on 5-ft models are presented and analyzed. The models were tested in calm water, and also in head and following seas. Tests included measurements of five components of force and moment. The draft, angles of attack and yaw, and model speed were varied. The results indicate that the S^3 is inherently stable, has low drag, and that an automatic control system could provide a nearly level ride in high sea states.

Introduction

The S^3 semisubmerged ship concept is a low waterplane, multihulled ship which basically consists of two parallel torpedo-like hulls, submerged to a depth of one to two diameters, and attached to an above-water platform by means of four widely spaced vertical struts. Horizontal fins and control surfaces on the hulls provide inherent dynamic stability and permit full control over pitch, heave, and roll.

The S^3 concept stemmed from designs of the author dating back to 1958. It was introduced at Naval Undersea Center (NUC) in 1968 to satisfy the need for a small, inexpensive support ship for a submer-

sible—one that could travel with large Navy ships in all sea states. Because *none* of the known ship types could fully satisfy all requirements, the S^3 was proposed. A preliminary analysis [1] indicated that the S^3 might also satisfy other NAVY needs. A comprehensive series of exploratory tests was consequently conducted on 5 ft models to investigate the drag, stability, and dynamic response of various configurations of the S^3. Only the drag and hydrodynamic coefficient results are presented here.

The complete test series consisted of approximately 500 tests conducted in the GENERAL DYNAMICS AEROMARINE TEST FACILITY model towing basin in San Diego, California, during August and September 1969. The towing basin is 315 ft long, 12 ft wide, and 6 ft deep. Additional tow tests were made in March 1970 in San Diego Harbor when one of the models was towed by a line to obtain additional data on drag.

This, paper is concerned primarily with the presentation of the *concept,* the *towing tank data,* and its *analysis.* A more complete description of the S^3 concept is presented in Reference [2] together with a description of other types of semisubmerged ship concepts.

DESIGN APPROACH

The design approach of the S^3 can be described while referring to Figure 1. Primary buoyancy is supplied by two streamlined hulls which are submerged to a depth of one to two diameters. The wave-making resistance and wave-induced forces are much less on these hulls than they are on conventional ship hulls. A *propeller* is placed at the end of each hull to utilize the boundary layer inflow to increase efficiency. Two vertical, surface-piercing, buoyant struts are attached to each hull. These struts provide hydrostatic stability in pitch, heave, and roll, a result of waterplane areas and spacing; they also provide hydrodynamic stability in yaw, a result of behavior as hydrofoils. Incorporation of a rudder into the aft strut provides improved maneuverability. The forward struts may also have rudders.

A submerged hull by itself is hydrodynamically unstable in *pitch,* the stablizing effect being proportional to velocity squared. Because the hydrostatic pitch stability provided by the struts is independent of speed, the combination becomes unstable above a certain critical speed, depending upon the configuration. Therefore, a horizontal tail surface is required to provide *pitch stability* at high speeds. This surface also improves both pitch damping and roll damping.

Incorporation of control flaps in the tail surface and of small controllable canard surfaces on the forward part of the submerged hulls provides effective control over heave, pitch, and roll in waves while maneuvering.

Because the relatively low wave drag of this configuration allows efficient high-speed operation of small ships, the S^3 appears to be best suited (in performance) for those combinations of size and speed between hydrofoil boats and conventional ships. Freedom of selection of strut size, lateral and longitudinal spacing, waterplane area, and horizontal fin sizes and locations allows virtually independent choice of pitch, heave, yaw, and roll response. The S^3 should provide good operational characteristics, whether or not automatically controlled. The addition of an automatic control system would permit the ship to operate smoothly in unusually high seas states.

TEST PLAN

Model Configurations

The models, constructed of wood and acrylic plastic, were made with interchangeable parts so that forms and sizes could be varied easily. Three basic models were tested. Drawings of Model A are in Figure 2. For this configuration, the deck platform is 52 inches long, and each hull has a horizontal

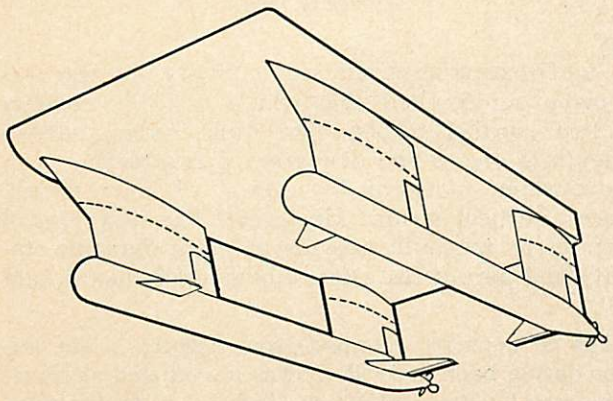

Figure 1. The NUC S^3 Semisubmerged Ship.

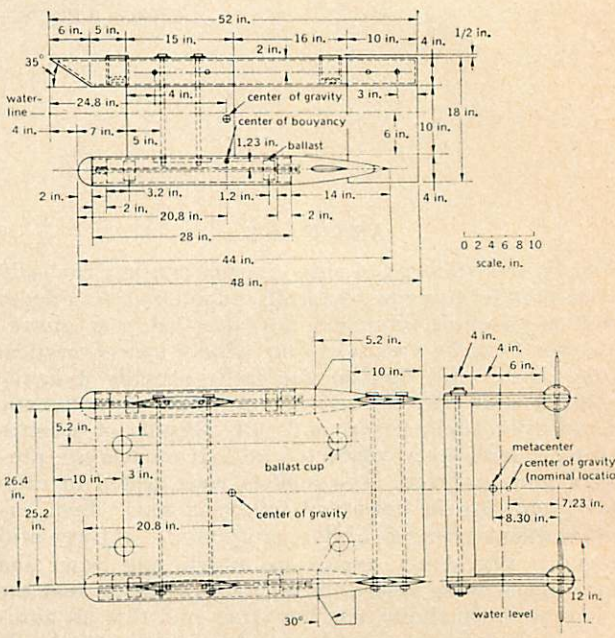

Figure 2. Model A.

TABLE 1
Model Weights, Metacentric Heights, and Natural Heave Periods.

Model Configuration	Hull Draft, d = 4 in.	Model Weight, lb	Metacentric Heigth Pitch, in.	Metacentric Heigth Roll, in.	Natural Heave Period, sec
A	0.0 d	32.0			
A	0.5 d	38.8			
A	1.0 d	41.7			
A	1.5 d	46.1			
A	2.0 d	49.1	0.52 to 1.49	0.33 to 1.48	2.25
A	2.5 d	52.1			
A + F + N	2.0 d	51.85	1.15 to 1.45	0.85 to 0.90	2.45
A + N	0.5 d	40.8			
A + N	2.0 d	51.3			
A + S	2.0 d	50.5 to 50.65	0.78	1.34	2.05
A + F	0.5 d	40.8			
A + F	1.0 d	43.7			
A + F	1.5 d	48.1			
A + F	2.0 d	51.5			
A + F	2.5 d	54.1			
B + N + F	1.0 d	59.08			
B + N + F	1.5 d	62.8			
B + N + F	2.0 d	66.05	1.45		2.6
B + N + F + S	2.0 d	69.30	0.9 to 1.5	1.9 to 2.4	2.4
C	0.5 d	38.1			
C	1.0 d	41.53			
C	1.5 d	44.9			
C	2.0 d	48.3			
C	2.5 d	51.85			
C + N	0.5 d	39.0			
C + N	1.0 d	42.43			
C + N	1.5 d	45.8			
C + N	2.0 d	49.2	1.39	1.47	
C + N	2.5 d	52.75			

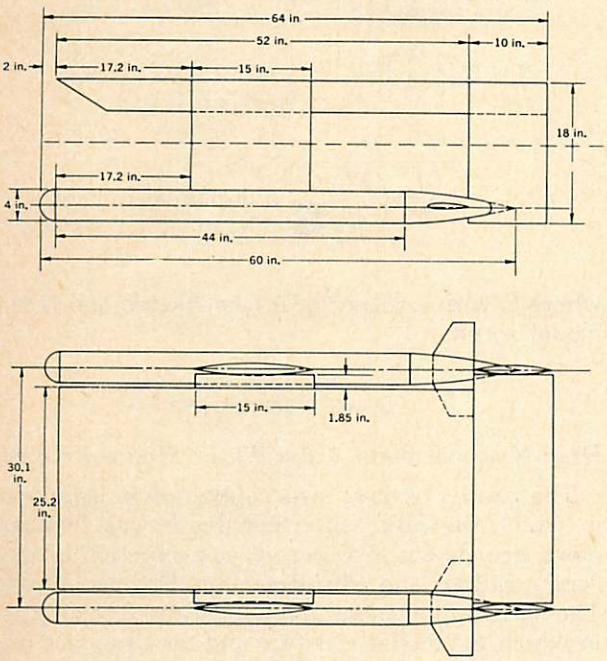

Figure 3. Model B.

fin and hemispherical nose. For Model B, the deck platform of Model A was lengthened by 10 inches and widened by 3.7 inches; the hulls were also lengthened by 16 inches as can be seen in Figure 3. Model C was the same as Model A *except that the fins were removed.* Although horizontal control surfaces near the noses, called canards, are embodied in the S^3 concept, they were excluded from tests of Models A, B, and C to isolate better the effectiveness of the stabilizing fin at the tail; also, this case simulates free-swinging canards.

Figure 4 shows drawings of the special parts used for Models A, B, and C consisting of a longer stabilizing fin (F), elliptical noses (N), and thicker forward struts (S). The designation is such that Model A becomes Model A+N by replacing the hemispheric noses with the *elliptical* noses. By also replacing the two horizontal fins with the longer modified fin and replacing the 1.8 inch thick forward

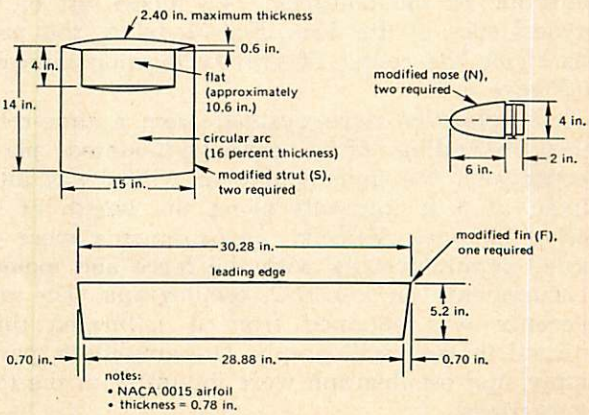

Figure 4. Special Model Parts.

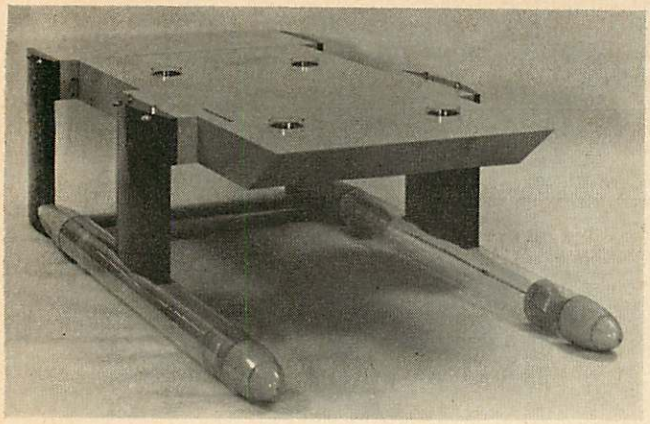

Figure 5. Photograph of Model B + N + F + S.

struts with the modified 2.4 inch thick struts, Model A becomes Model A+N+F+S. Figure 5 is a photograph of Model B+N+F+S. Fine grains of sand that form a circle around the hull noses and saw-toothed-edge strips of thin tape on each side of the leading edge of each strut were added for turbulence stimulation.

The draft and center of gravity were changed by placing *lead ballast* in the hull, in the deck ballast cups, and on top of the deck. DRAFT is defined as *the hull centerline depth,* specified in terms of HULL DIAMETERS. Weights of the models for various configurations and drafts in fresh water are given in Table 1. These weights were used in the determination of FROUDE NUMBERS, F_∇.

Test Outline

With the model fully restrained, towing tests were made using various model configurations at speeds of 2 to 15 ft/sec at five different drafts in smooth water and in head and following waves. Drag, side, and lift forces and pitching and yawing moments were measured. The angle of attack in pitch and yaw was also varied. The tests were conducted in fresh water at 70° to 74°F.

Three force guages were used to measure drag D, lift L, and pitching moment M, or alternatively, the drag, side force Y, and yaw moment N.

Moments were measured about a point on the centerline of the platform, 24.8 inches aft of the forward edge of the deck. For Model A, this point was *above* the center of gravity location indicated in Figure 2.

Test velocities were derived from a time-referenced recording of a carriage-mounted photoelectric cell, the light source of which was interrupted at 5 ft intervals along the length of the towing channel. Velocity measurements were recorded simultaneously with the force and moment measurements on a C.E.C. oscillograph. The time reference was obtained from a calibrated timer external to the oscillograph. The amplifiers, power supply, and oscillograph were mounted on the towing carriage.

Desired wave heights and lengths were verified by photographing the wave profile against a grid located on the inside wall of the towing basin and by making direct periodic measurements.

Data Reduction

The experimental data were reduced to coefficient form to make the data non-dimensional, and therefore directly applicable to different ship sizes. The characteristic length was selected to be the one-third power of the displaced water volume = $W/\rho\ g$, where W is the model weight; ρ is the mass density of water; and g is the acceleration of gravity. This length selection permits the various configurations to be more meaningfully compared. It also permits the test results to be more readily compared with those of other ship types where total ship weight, and not ship length, is the primary parameter.

The following definitions will be used in the remainder of this report:

$$D = C_D\left(\frac{W}{\rho g}\right)^{2/3}\frac{\rho U^2}{2} = \text{drag (+aft)}$$

$$L = C_L\left(\frac{W}{\rho g}\right)^{2/3}\frac{\rho U^2}{2} = \text{lift (+up)}$$

$$Y = C_Y\left(\frac{W}{\rho g}\right)^{2/3}\frac{\rho U^2}{2} = \text{side force (+ starboard)}$$

$$M = C_M\left(\frac{W}{\rho g}\right)\frac{\rho U^2}{2} = \text{pitching moment (+ bow up)}$$

$$N = C_N\left(\frac{W}{\rho g}\right)\frac{\rho U^2}{2} = \text{yaw moment (+ bow starboard), and}$$

$$F_\nabla = \frac{U}{\sqrt{g\left(\frac{W}{\rho g}\right)^{1/3}}} = \text{displacement FROUDE NUMBER,}$$

where C with a subscript is a coefficient and U is the model speed.

DRAG COEFFICIENT

Drag Measurements, Calm Water, Nominal Draft

The results of drag tests conducted in calm water, in which the hull centerline depth was two diameters, are shown in Figure 6 as a function of model configuration and displacement FROUDE NUMBER. The dashed line refers to towline drag measurements in which the model was free and the drag was measured with a spring scale. The dashed line data (free model) are most accurate at the lower half of the FROUDE NUMBER range. The restrained data points are most accurate at high FROUDE NUMBERS; their scatter at low FROUDE NUMBERS indicates poor accuracy below $F_\nabla = 0.80$. (Notice that the values of F_∇ are much larger than the more conventional Froude numbers that are based on model length.)

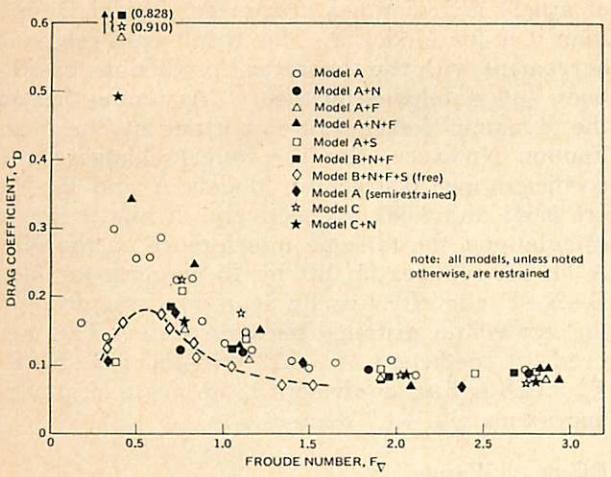

Figure 6. The Drag Coefficient as a Function of Froude Number for Various Models. NOTE: The Hull centerline is two diameters deep.

Examination of the data at higher Froude Numbers shows that C_D approaches a constant and is not significantly affected by configuration. The length, Reynolds Number, of the model at the highest test speed was 7.5×10^6. Roughness strips were added to the hulls and struts to produce a turbulent boundary layer. The measured drag data are reasonably accurate, but tests on a larger model would provide better values assuming that the larger model is well streamlined and that all surfaces are smooth. Because the skin friction portion of the drag coefficient reduces with increasing Reynolds Number, the drag coefficient will be significantly *lower* for large ships. However, the wave-drag and strut-spray-drag portions of the drag coefficient are essentially a function of model form and Froude Number. Thus, these portions will change only with ship size because the ship form will change with ship size and mission. The dashed line in Figure 6 shows that wave drag reaches a peak at approximately $F_\nabla = 0.55$ for Model B + N + F + S. The wave drag is very small, above $F_\nabla = 1.3$, and is also small below $F_\nabla = 0.3$. Therefore, the region of maximum wave drag is not in the most important operating region of naval ships. Table 2 shows the relationship between ship weight, speed, and displacement Froude number.

TABLE 2

Ship Speed as a Function of Ship Weight and Displacement Froude Number.

		Speed, knots				
F_∇	Model B + N + F	50 tons	500 tons	2,000 tons	10,000 tons	50,000 tons
0.25	0.8	2.9	4.3	5.4	7.1	9.3
0.50	1.7	5.9	8.6	10.9	14.1	18.5
1.0	3.4	11.7	17.2	21.7	28.3	37.0
1.5	5.1	17.6	25.8	32.6	42.4	55.5
2.0	6.8	23.4	34.4	43.4	56.6	74.0
3.0	10.2	35.1	51.6	65.1	84.9	111.0

Analysis of the drag data indicates that the value of C_D for prototype ships, after correcting for Reynolds Number, will lie between 0.04 and 0.05 at cruise and top speed, especially if spray rails, as introduced in Reference [3], are utilized. Thus, the drag would be less than well-designed monohulls. Also, recent theoretical work by R. B. CHAPMAN shows that the low-speed wave drag hump can be considerably reduced by simple strut and hull form changes.

Effect of Operating Draft

Model data as shown in Figure 7 indicate that the drag coefficient reduces with operating draft. A typical drag reduction is 20 percent between a hull centerline draft of two diameters and a draft of 0.5 diameter at the various test FROUDE NUMBERS. This reduction is apparently caused by reduced strut friction drag and reduced strut wave or spray drag as the strut immersion approaches zero.

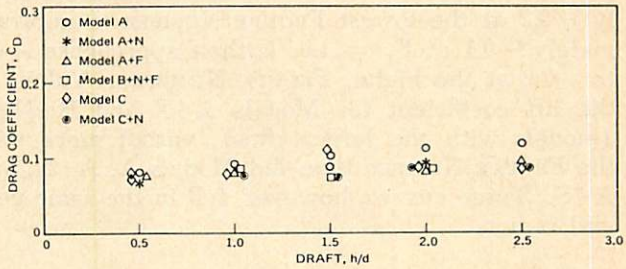

Figure 7. The Drag Coeffiicent as a Function of Draft for Various Configurations at $F_\nabla = 1.90$.

Effect of Waves and Trim Angle

Data gathered on several configurations in 2 × 40-in., 4 × 40-in., 4 × 80-in., and 6 × 120-in. waves show no significant effect of waves on mean drag, relative to calm water. Similarly, data gathered on different configurations at a pitch of 3 degrees at yaw angles of 2 and 4 degrees show no significant change in C_D from the zero trim angle. The variation of C_D in waves is called $\pm\Delta C_D$, and indicates the magnitude of surge force. The value of ΔC_D generally varied from 0.020 at $F_\nabla = 0.8$ to approximately 0.002 at $F_\nabla = 3.0$ for all models tested in 4 × 80-in. waves, in either head or following seas. The data scatter at $F_\nabla = 0.4$ was too great to obtain meaningful information.

LIFT COEFFICIENT

In fully restrained tests, the lift coefficient, C_L, was measured for model configurations A, A + N, A+F, A+S, B+N+F, C, and C+N as a *function* of draft, FROUDE NUMBER, angle of attack α, and wave height and direction.

Effect of Draft

For most FROUDE NUMBERS, particularly the higher ones, the effect of various design drafts on the lift coefficient was negligible and within the data scatter

when the draft was one diameter or greater. At a draft of 0.5 d (that is, hull tops at the surface), the lift coefficient was reduced in value by approximately 0.07. Note that strut buoyancy produces a calculated change in C_L of $0.076/F^2$ per inch for Model A and $0.070/F_\nabla^2$ for Model B+N+F. This change is the only heave stabilizing force, and it is adequate to stabilize fully the models over the range of test FROUDE NUMBERS.

Effect of Froude Number

The variations of the lift coefficient with FROUDE NUMBER are shown in Figure 8; the hull centerline depths are two diameters. The value of the lift coefficient for Models C and C+N (models without stabilizing fins) remained essentially *constant* at −0.05 and independent of FROUDE NUMBER. For Models A, A+N, and A+S (models with intermediate-size fins), the values varied from approximately −0.2 at the lowest FROUDE NUMBER to approximately −0.1 at $F_\nabla = 1.0$; it then approached −0.1 to −0.2 at the higher FROUDE NUMBERS. Values of the lift coefficient for Models A+F and B+N+F (models with the largest fins), varied more with the FROUDE NUMBER than did Models A, A+N, and A+S. These curves, however, fell in the same general region.

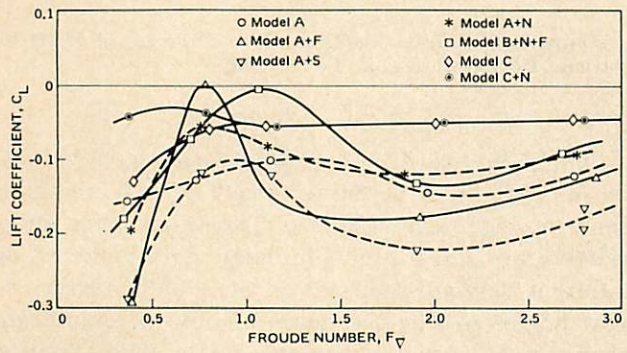

Figure 8. The Lift Coefficient as a Function of Froude Number in Calm Water.

Effect of Angle of Attack

The angle of attack was set at 0 and 3 degrees for two of the models. The change in the lift coefficient per degree for Model A was reduced from approximately 0.06 at $F_\nabla = 0.4$ and 0.8 to 0.04 at $F_\nabla = 2.0$ where it leveled out. The change in lift coefficient per degree for Model B+N+F was reduced from approximately 0.20 at $F_\nabla = 0.4$ to 0.07 at $F_\nabla = 1.1$ where it again leveled out. The near-surface effects, the strut displacement, and wave-making effects on the *lift coefficient* per unit angle of attack were most significant below $F_\nabla = 1.1$ and more pronounced on Model B+N+F which had the largest stabilizing fin. At the higher FROUDE NUMBERS, where wave-making is small and water flow is more predictable, the change in lift coefficient with angle of attack is 1.75 times greater for Model B+N+F than it is for Model A. This result is in reasonable agreement with the theoretical predictions based on body and stabilizing fin theory. Assuming that only the dynamic forces are important at the higher FROUDE NUMBERS, the theoretical changes in lift coefficient per degree for Models A and B+N+F are 0.041 and 0.081, respectively. In the theoretical calculations, the tailcone interference on the Model A fin lift reduces fin lift by 15 percent; for Model B+N+F, the effective fin span was assumed to be the centerline distance between hulls. The measured lift coefficient of −0.12 for Model B+N+F at $F_\nabla = 2.8$ is thus equivalent to an angle of attack of approximately −1.7 degrees.

Effect of Waves

The average values of the lift coefficient in waves were generally similar to the calm-water case for all configurations. The variation in the lift coefficient, called $\pm\Delta C_L$, is important in determining control effectiveness of the S[3] because the control surfaces must provide an equal and opposite force to obtain level flight in waves. Configurations A, A+F, A+S, B+N+F, and C were tested in 4 × 80-in. head and following waves. Figure 9 presents the data on the variation of the lift coefficient as a function of FROUDE NUMBER. Data show that the variation in the lift coefficient is generally relatively small, and has a maximum value in following seas of 0.3 to 0.4 at $F_\nabla = 0.4$. Above $F_\nabla = 1.0$, it is less than 0.21. Its value is smaller in head seas than in following seas, and is negligible (that is, less than 0.02) for FROUDE NUMBERS greater than 1.0. Contrary to expectations, there appears to be no significant trend of the variation in lift coefficient with fin size, possibly because of data scatter. Additional data were taken in 2 × 40-in. and 6 × 120-in. waves for Model A. These data tended to correlate with the data for the 4 × 80-in. waves after adjustment for wave size. Significant data scatter, however, was again present.

Theoretically, small canard control surfaces near the noses and flaps in the tail stabilizer can fully counteract the measured changes in lift and provide a level ride. For example, a 30 percent chordlength flap in the stabilizing fin would provide $\Delta C_L = 0.2$ with a deflection of only 5 degrees. Alternatively, a pair of canard fins with a span of only 4 in. and an average chord of 4 in. would have to be deflected approximately 16 degrees to provide a $\Delta C_L = 0.2$. Larger canards, of course, would require less deflection.

PITCHING MOMENT COEFFICIENT

The pitching moment coefficient, C_M, of several configurations was measured as a *function* of draft, FROUDE NUMBER, angle of attack, and wave motion.

Effect of Draft

Draft has only a small effect on the pitching moment coefficient, and is noticeable only at hull cen-

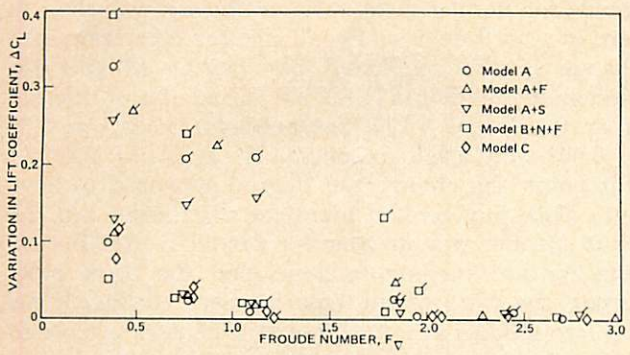

Figure 9. Effect of Waves on Changes in the Lift Coefficient as a Function of Froude Number. NOTE: The flagged data points represent following seas, and the unflagged data points head seas, 4 x 8 inch waves.

terline drafts of 0.5 to 1.5 diameters. The models tested were A, A+N, A+F, B+N+F, C, and C+N.

Effect of Froude Number

Figure 10 shows the values of the pitching moment coefficient as a function of FROUDE NUMBER for the various models tested at a draft of two diameters. The effect of FROUDE NUMBER was noticeable up to values of 1.8 or 2.0. The pitching moment coefficient for Models C and C+N was approximately −0.1 (bow down), and varied relatively little with FROUDE NUMBER—perhaps because the models had no stability fins. Analysis of the pitching moment coefficient indicates that the negative value is largely caused by the drag force acting on the submerged model parts. Because the moment is measured at a point just above the model deck, the value produced by drag is:

$$(C_M)\ \text{drag} = -\frac{D\, z_D}{V(\rho/2)U^2} = -C_D \frac{z_D}{V^{1/3}} = -1.2\, C_D$$

where z_D is the vertical distance between the balance attachment point and the center of drag force. Because $C_D = 0.1$ at the larger FROUDE NUMBERS, the value of C_M due to drag is -0.12, approximately the value measured for Model C. In a self-propelled model, the pitching moment coefficient would, therefore, be larger by approximately 0.12. The value of the pitching moment coefficient for Models A, A+S, and A+N (intermediate fin size) varied more with FROUDE NUMBER; the largest variation occurred for Models A+F and B+N+F. For these models, the pitching moment coefficient exceeded 0.2 at $F_\nabla = 0.4$; fell to −0.20 at $F_\nabla = 1.0$; and then rose to the region of 0 to 0.1 at $F_\nabla = 1.8$ and above.

The earlier analysis of the lift can now be used to show that the pitching moment coefficient can be completely cancelled by means of control surfaces located near the front and rear of the hulls. If the control surfaces are a distance l_c apart, and if C_L is their lift coefficient, then they can generate a pitching moment coefficient of:

$$C_M = \frac{l_c\, C_L V^{2/3}(\rho/2)\, U^2}{V\,(\rho/2)\, U^2} = C_L \frac{l_c}{V^{1/3}}.$$

Therefore, to counteract a $C_M = 0.2$ on Model B+N+F, the lift coefficient must be approximately 0.05. As previously shown, this value can easily be generated by small control surfaces.

Effect of Angle of Attack

Models A and B+N+F were tested at attack angles of 0 and 3 degrees. Although the data are scattered to some extent, they indicate a pitching moment coefficient per degree of approximately −0.033 (nose down) for Model A and approximately −0.10 for Model B+N+F. The calculated values of the pitching moment coefficient per degree for the two models at higher FROUDE NUMBERS are −0.027 and −0.14, respectively, assuming that only dynamic forces are important and that lift is generated at the hull noses and the stabilizing fins. The pitching moment, caused by strut buoyancy change as the angle of attack increases, is independent of speed and provides a strong stabilizing influence.

An analysis of the measured values of the pitching moment coefficient in Figure 10, combined with

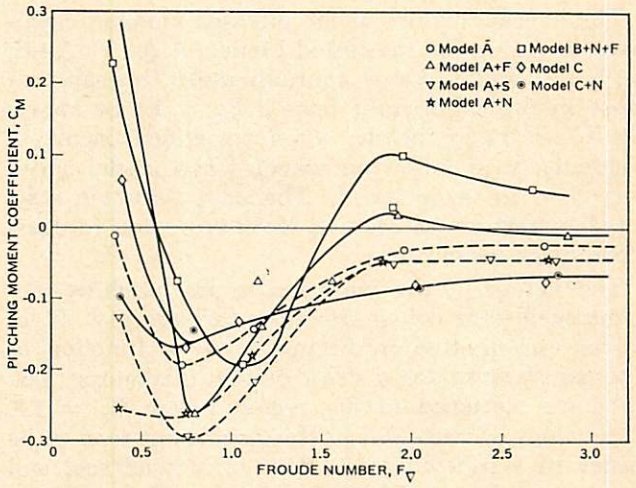

Figure 10. The Pitching Moment Coefficient as a Function of Froude Number in Calm Water.

the above experimental values, shows that the pitch of a free, uncontrolled, and unpowered model running at $F_\nabla = 2.0$ or above, would be approximately 1.0 degree for Model B+N+F or approximately −1.0 degree for Model A. The largest pitch, which would occur near $F_\nabla = 1.0$, would be −2.0 degree for Model B+N+F or −6.0 degrees for Model A. If the model was free and self-propelled, the thrust vector acting along the hull centerline would pitch the nose of the model above these values by an amount equal to approximately 1.2 degrees for Model B+N+F or 3.6 degrees for Model A; each calculation is valid for FROUDE NUMBERS above 1.5. Thus, the data suggest that the largest fin, F, is best, and should be placed at a small fixed trim angle to minimize the net pitching moment of the model at the

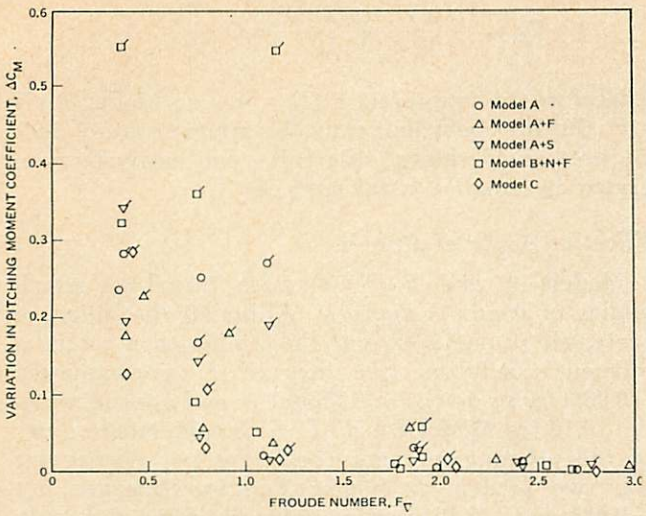

Figure 11. Effect of Waves on Changes in the Pitching Moment Coefficient as a Function of Froude Number. NOTE: The flagged data points represent following seas and the unflagged data points head seas.

higher FROUDE NUMBERS.

Effect of Waves

The average values of the pitching moment coefficient in waves for the tested Models A,A+F, A+S, B+N+F, and C were approximately the same as those in the calm-water tests if $F_\nabla = 1.0$ or above. At $F_\nabla = 0.7$ or below, some variations occurred, particularly in following waves when model speed was close to wave speed. The data were too scattered in this lower FROUDE NUMBER region to draw meaningful conclusions.

The values of the variation in the pitching moment coefficient, when traveling through 4 × 80-in. waves, are plotted in Figure 11 as a function of FROUDE NUMBER for a draft of two diameters. The data are scattered in the region below $F_\nabla = 1.2$. The values of variation in this coefficient tend to be larger in a following sea than in a head sea, and reach a maximum of 0.30 to 0.55 at low FROUDE NUMBERS. The maximum values in head seas vary from 0.12 to 0.32. Above $F_\nabla = 1.7$, the values are relatively small, and always less than 0.06. According to theory, the largest moment change, $\Delta C_M = 0.55$, can be controlled by control surfaces at the nose and tail, each generating a $C_L = 0.14$. This value can be developed by relatively small control surfaces and deflections.

YAW COEFFICIENTS

The yaw force and moment were measured as a *function* of F_∇ for Models A+N+F and B+N+F at yaw angles, β, of 0, 2, and 4 degrees for the nominal draft of two diameters in calm water.

Yaw Force Coefficent

The sideforce coefficient data, C_Y, exhibited smooth trends for both models. The coefficient was close to zero at $\beta = 0$ degrees for all FROUDE NUMBERS. The change in the coefficient per degree of yaw for Models A+N+F and B+N+F varied almost linearly from 0.180 and 0.100, respectively, at $F_\nabla = 0.35$ to 0.031 and 0.025, respectively, at $F_\nabla = 2.6$. At this point, the change per degree appeared to level out. Both models had identical strut sizes, but the strut spacing was greater for Model B+N+F. Assuming that the struts developed the same sideforces, the ratio of the yaw moment coefficient for the two models at large FROUDE NUMBERS is close to their reference areas as theory indicates.

Calculating the hull nose lifts and assuming that the strut aspect ratios at large FROUDE NUMBERS are based on their wetted heights, calculations show that the experimental results agree with theory if the sideward downwash from the front struts completely cancels the sidefore of the aft struts. Because the aspect ratio of the front struts is very low, this result is reasonable. In theory, the angle of downwash at the aft strut is $\beta_2 \doteq \beta/2AR$ for aspect ratios AR less than 1.0. Consequently, because AR = 1/2, the downwash angle $\beta_2 \doteq \beta$, leaving zero lift.

Why C_Y is much larger at the lower FROUDE NUMBERS (that is, increased by a factor of 4 to 6) is not known. However, it is known that the water surface at low F_∇ acts as a wall, doubling the effective strut aspect ratio which nearly doubles the front sideforce and slightly reduces its downwash. However, even this is not enough to fully explain the change. It is probable that complex wave-strut interaction is occurring, making predictions difficult at the lower F_∇.

Yaw Moment Coefficent

Data for the yaw moment coefficient, C_N, exhibit smooth trends with F_∇ for Model B+N+F, except at the lowest test value where the data scatter. (The data for Model A+N+F show considerable scatter at most values of F_∇.)

Data for Models B+N+F and A+N+F show that the respective changes in C_N per degree of yaw are 0.025 and 0.072 (overturning moments), respectively, at $F_\nabla = 0.7$ to 0.0 and 0.035 at $F_\nabla = 2.6$. The larger values for Model A+N+F are reasonable because the front struts on Model A+N+F are farther forward. Although the static hydrodynamic moment coefficients indicate an overturning moment, both models are dynamically stable in yaw because of dynamic effects.

An analysis of the high FROUDE NUMBER data for C_N indicates that the sideforce generated by the aft strut is 0.17 of its calculated value for Model B+N +F and −0.16 for Model A+N+F. Thus, these results generally agree with the yaw force data, and suggest complete downwash on the aft struts.

CONCLUSIONS

The S^3 semisubmerged ship concept appears to be

stable in all respects without the use of controls. At the design cruise and top speeds, the drag is less than conventional monohulls. The test data indicates that heave, pitch, and roll motion in waves should be small because of lack of large forces and moments. The data also indicate that the addition of small control surfaces and an automatic control system would provide a near-level ride in very high waves. Contrary to conventional ships, large waves do not appreciably increase the drag.

REFERENCES

[1] Lang, T. G., "A New Look at Semisubmerged Ships for the Navy", Internal NUC Report, TN-251, May, 1969.

[2] Lang T. G., "S^3, New Type of High-Performance Semisubmerged Ship," Naval Undersea Research and Development Center, San Diego, Calif., ASME, Paper No. 71-WA/UnT-1, August 1971.

[3] Chapman, R. B., "Spray Drag of Surface-Piercing Struts", Naval Undersea Research and Development Center, NUC TP-251, 1971.